Rotating Electrodes for Use in Electrodeposition Process Control

(The 36th William Blum Lecture)

By Dr. David R. Gabe

The characteristic properties of the Rotating Cylinder Electrode of specific interest to the electroplating community are described and the author's own research contributions to our current state of knowledge are discussed under the following topic headings: Electrode Characteristics, Use for Voltammetry, RCE Reactor Theory, Process Simulation, Electrodeposit Morphology Diagrams.

In acknowledging the honour accorded me by the American Electroplaters and Surface Finishers Society in bestowing the Scientific Achievement Award for 1995, I am conscious of the historical inheritance, not only through the name of William Blum, with whom it is associated, but also of the previous recipients, going back to 1958, whose names make a daunting roll call of the good and the great of our profession. William Blum was a great founder of the scientific tradition of our profession through his association with the AESF and the National Bureau of Standards, as well as through his scientific publications, including a book and a laboratory test cell of worldwide fame. The Blum throwing power cell, like the Hull Cell, has been seen to suffer some minor drawbacks while remaining true to its original intent (*i.e.*, they are both essentially static), and this is the theme that I wish to explore in this lecture.

Rotating electrodes have their own historical tradition. While the Rotating Disc Electrode (RDE) was undoubtedly invented by V.G. Levich, the Rotating Cylinder Electrode (RCE) has a less well-defined history. I was introduced to it via my connection with tin-plate research, through the papers of Donald Swalheim (1944) and Kenneth Graham (1963), so the American pedigree of this electrode geometry is assured![1,2] The problem that I was considering was essentially one of laboratory simulation (*i.e.*, design of a cell), in a compact style for laboratory convenience, of the strip-plating process of tin-plate manufacture, where the substantial agitation is of a badly specified and controlled turbulent variety.

Table 1
Electroplating Applications Studied with the RCE

Preplating and pretreatment for tinplate production
Mass-transfer analysis of the RCE; Cu, Sn
Onset of dendritic growth; Cu, Sn, Ag, Ni, Zn
RCE reactor theory; electrowinning
Enhancement of mass transfer through surface roughness
RCE and RConE electrodes for current density cells
Enhancement of mass transfer by two or more flows
Process simulation
Deposit morphology control
Multilayered coatings (CMA techniques)

Instinct took Swalheim and Graham to the RCE, and time has shown that instinct absolutely appropriate.

The RCE can be used in a number of fields beyond today's territory—corrosion, turbulent fluid flow simulation and definition, viscometry, etc.—and those interested in such aspects are referred to three major reviews.[2-5] The range of topics that I and my coworkers have explored, using the RCE, is summarized in Table 1.

Electrode Characteristics

Rotating electrodes are primarily employed to impose forced convection on an electrode reaction, to negate vagaries of free convection that can arise as a result of thermal and density changes in the vicinity of the electrode/electrolyte interface. An associated virtue is that the rotation provides an excellent quantitative measure of the agitation employed, thereby enabling mass-transfer-controlled reactions to be adequately investigated. It is customary to use model reactions for this purpose, typically ferri/ferro-cyanide or acid copper sulfate solutions.

The type of electrode employed is selected according to need, but always to exploit the limiting-current experimental data in a relevant flow regime. A number of variables may be involved:

$$i_L = f (D, \nu, C, U, d)$$

Consequently, most electrodes could be used in analytical applications, such as voltammetry, in which the main purpose is to measure D or C, where

- D is ion diffusion coefficient
- ν is solution viscosity
- C is ion concentration
- U is electrode rotation rate
- d is critical dimension (*e.g.*, electrode diameter)

In this type of work, the main criterion is obtaining a stable and relevant convective motion, the relevance relating to other and possibly industrial applications. Accordingly, the RDE is a preferred geometry for laminar flow regimes and the RCE for turbulent regimes. The RConE and RHSE are actually truncated modifications of the RDE and, consequently, do not offer radically different options (see Fig. 1).

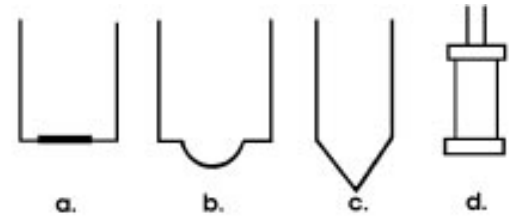

Fig. 1—Types of rotating electrode.

Table 2
Types of Rotating Electrodes

Discs (RDE)	Single isolated discs	RDE, RRDE for electroanalysis
	Confined gap cells	Capillary gap and pump cells
	Multiple stacked discs	Trickle tower reactors
Cylinders (RCE)	Confined cell	Viscometry, batch electrochemical cells, corrosion/erosion cells voltammetry
	Flow-through cells	Continuous reactors
	Cascade cells	Continuous reactors
Cones (RConE)	Throwing power cells	Current distribution assessment
Spheres, Hemispheres (RH/SE)	Modified RDE	Voltammetry

RHSE, especially for voltammetry, where the more uniform current distribution below the limiting-current density is claimed to offer increased versatility for studying high-rate corrosion processes.

The characteristics of the four main categories of rotating electrode are summarized in Tables 2 and 3, and the most useful mass transfer relationships are given in Table 4.

Table 3
Comparison of Rotating Electrodes

$Sh = const\ Re^n$

Rotating Electrode System	n laminar	n turbulent	Transitional Re_{crit}
Disc (RDE)	0.50	0.90	10^5
Cylinder (RCE)	0.33	0.67	2×10^2
Hemisphere	0.50	0.67	2×10^4
Inverted cone	0.45	0.88	6×10^4
Upright cone	0.48	0.93	1×10^5
Annular flow	0.33	0.58	2×10^3

Table 4
Mass Transfer Relationships

RDE laminar	$i_L = 0.62\ zFCD^{2/3}\nu^{-1/6}\omega^{1/2}$	$Sh = 0.62\ Re^{1/2}Sc^{1/3}$
RCE turbulent	$i_L = 0.079\ zFCD^{0.64}\nu^{-0.34}U^{0.7}$	$Sh = 0.079\ Re^{0.7}Sc^{0.33}$
RConE laminar	$i_L = 4\ zFCD\omega^{0.48}l^{1.48}\nu^{0.48}(\sin\alpha)^{0.48}$	$Sh = 4.0\ Re^{0.48}$
RHSE laminar	$i_L = 0.474\ zFCD^{2/3}\nu^{-1/6}\omega^{1/2}$	$Sh = 0.474\ Re^{1/2}Sc^{1/3}$

It can be noted that the RCE is markedly different, offering a number of specific characteristics:

- turbulent flow domination at relatively low rotation rates
- uniform current distribution when employing a concentric anode format
- uniform mass transfer over the cylindrical surface
- an equipotential surface capable of allowing complete potentiostatic control
- rough surfaces that can enhance mass transfer
- superimposed axial flow that can promote mass transfer without being rate-controlling.

In practical terms, the real choice is between the laminar RDE and the turbulent RCE. Special cases, however, have been argued for other geometries; in particular, Gabe *et al.*[6] and Landolt *et al.*[7] have demonstrated the virtues of the RConE and RCE for current distribution studies in the format of modified Hull cells. Chin[8] has explored the value of the

Use for Voltammetry

Voltammetry involves use of polarization data in general, but for quantitative analysis, it necessarily concerns concentration polarization and the relationships that can be exploited (see Table 4). A number of options exists for constant rotation velocity (U) determinations.

For the RDE, i_L is proportional to C, $D^{0.67}$, $\nu^{-0.166}$
For the RCE, i_L is proportional to C, $D^{0.64}$, $\nu^{-0.34}$

It should be noted that in both cases, the proportionality to concentration C is direct, but to diffusion coefficient D and kinematic viscosity ν it varies in each case.

Clearly, these are so similar mathematically that other considerations must influence the preferred technique. In practice, the RDE in laminar flow is widely used as a stable hydrodynamic system of long-established, proven capability and proven quantitative relationship. The RCE in turbulent flow, however, is equally appropriate, but less widely used by analytical chemists.

Although not strictly part of the topic covered here, the analogous technique of polarography should not be forgotten, because it also makes use of diffusion-limiting currents, but in this instance at the Dropping Mercury Electrode (DME). While the DME has no equivalent hydrodynamic dimension, it has a thermodynamic dimension, because the metal is electrodeposited into a mercury amalgam effectively at zero activity, whereas at the RDE and RCE, it is usually deposited at unit

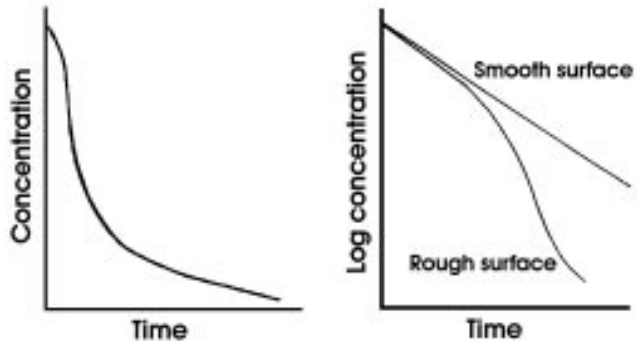

Fig. 2—Concentration-time relationships: (a) exponential decay in batch operation; (b) logarithmic graph for smooth and rough surfaces.

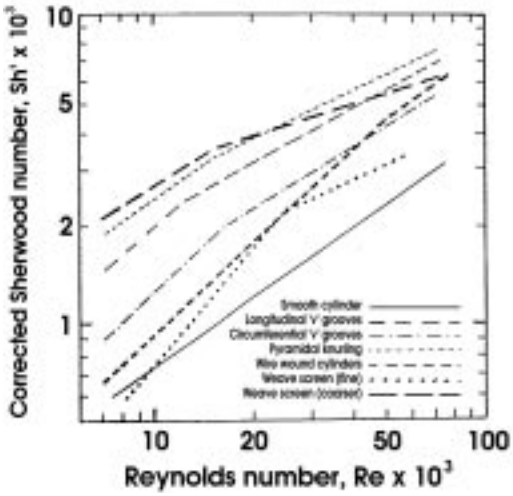

Fig. 3—Enhancement by roughness: Mass transfer correlations (Sh/Re) for several types of roughness on a RCE, using acid copper deposition (after Makanjuola and Gabe).

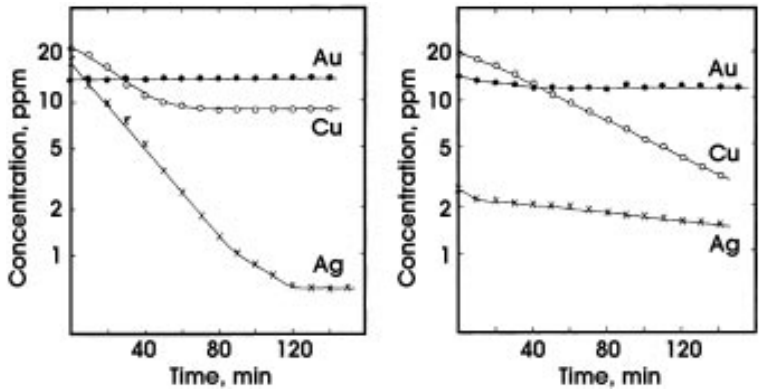

Fig. 4—Potentiostatic separation with the RCE (after Walsh and Gabe).

activity; as a result, this gives it substantial technical advantage for base metals and mixed metals of varying ionic charge.

RCE Reactor Theory

An electrochemical reactor is designed to produce high-reaction product yields at high efficiency, either at anode or cathode, as a consequence of the passage of current. It should also be compact, convenient and economical in use. The RCE has a number of opportunities in this context, but cathodic recovery, or electrowinning, of metal from industrial effluent and mine leach liquors is the application primarily considered here. The technical requirements of a RCE reactor are as follows:

1. Turbulent flow to develop high mass-transfer coefficients, K_L.
2. High cathode surface area to maximize the limiting *current* at flow-controlled, *limiting-current density*. Rough electrodes, therefore, offer deposition enhancement.
3. Small compact cells are desirable, in either batch or continuous mode of operation.
4. Metal is recoverable as a coherent cathode deposit or as a scrapeable dendritic powder.
5. Cathode separation of metals by selective potentiostatic-controlled deposition is possible.
6. Low parasitic energy consumption (*i.e.*, through pumping, rotation, heating etc.), can be feasible.
7. Metal is recovered from low-concentration solutions at relatively high current efficiencies.

The RCE meets all these requirements to varying extents and examples will be described to illustrate these propositions.

Reactor theory and practice related to RCE-type cells have been discussed in detail in two papers,[9,10] but some of the important aspects will be described. Reactor performance can be characterized in a number of ways, depending upon the purpose to which the reactor is directed. Design criteria describe performance according to shape, size and throughput ratios, some of which are given in Table 5. The design criteria employed for a specific need will depend upon the critical design factor, typically reactor compactness, energy efficiency during use, volume throughput etc. When the reactor is employed for metal recovery from waste solutions, leach liquor, effluent and the like, recovery conversion factors can be defined; Table 6 lists the mathematical expressions for four modes of reactor operation.

A practical approach to recovery performance makes use of the rate at which metal concentration falls with time in the recovery flow circuit. In an ideal batch reactor, the concentration will fall exponentially with time, and this is used as the yardstick for actual performance. Several factors will affect the departure from the ideal; for example, at very low concentrations of metal in solution (<50 ppm) current efficiency will fall below 100 percent and change with both residual concentration and hydrodynamic conditions in the reactor. A more important situation arises as a result of using the reactor at as high a current as possible to maximize the yield; at the limiting current, dendritic or powdery deposit growth takes place and the cathode surface becomes markedly roughened. This offers two bonuses to the operator. First, flow patterns at the surface become more turbulent and, if the powder becomes detached, entrainment occurs as a form of con-

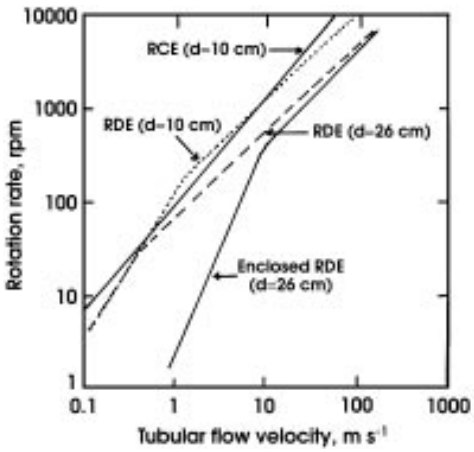

Fig. 5—Graph of RCE and RDE rotation rate against tubular flow velocity, demonstrating flow equivalence in the turbulent regime for a corrosion process (after Heitz).

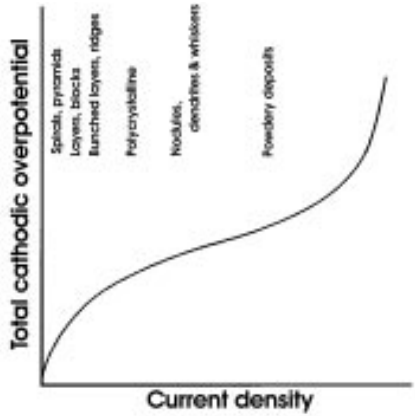

Fig. 6—Cathodic polarization diagram showing ranges of characteristic growth modes.

Table 5
Reactor Performance Compared

Cell type	Electrode area / Reactor volume (cm^{-1})	Space-time yield (Goodridge) Y_{ST} (hr^{-1})	'Specific' energy consumed (Kreysa) E^e_s (KWh m^{-3})	Normalized space velocity (Kreysa) p^n_s ($dm^3\ dm^{-3}\ hr^{-1}$)
Filter press	0.3–1.7	0.12–0.68	—	—
Capillary gap	1.0–5.0	0.4–2.0	—	—
RDE	1	4	—	—
RCE	0.1–1	0.4–4	1.5	20
Packed bed	10–50	4–20	0.12	28
Fluidized bed	20–100	8–40	0.27	30
Swiss roll	20–50	—	1.0–1.2	12–20
Rolling tube	—	—	14.2	0.4
Rotating packed bed	—	—	0.13	250

tinuous metal removal. Second, the increased cathode surface area enables the reactor performance to improve apparently beyond that predicted by the exponential relationship. Figure 2 illustrates this enhanced recovery performance, which can lead to recovery times, in batch mode operation, being reduced by a factor of 2–3, or from three hr to one!

Continuous operation, especially in a series of reactors or in a "cascade" cell, can raise the effectiveness of recovery performance markedly. The data in Table 7 show how a six-cell series, each individual cell or compartment offering 50-percent recovery, can give 98.4 percent overall recovery and a residual metal concentration of 1.5 ppm, rather than 50 ppm when the initial concentration is 100 ppm, which could be a typical drag-out level in an electroplating plant.[11]

Such roughness can either develop naturally, as a consequence of diffusion-limiting electrodeposition yielding dendritic growths, or may be pre-arranged. Makanjuola investigated a large variety of designer-roughened electrodes for this purpose.[12] They can be compared in terms of degrees of enhancement for particular flow velocities or Reynolds numbers, as in Fig. 3, and an optimum roughness selected for a given reactor design and operating conditions.

Selective separation of mixed metal solutions is often desirable, not only as a consequence of using alloy plating solutions, but also when effluent streams are mixed, or when pickle wastes are encountered, or in treatment of leach liquors. Selective deposition is possible, using the RCE, because of its equi-potential surface and, thereby, potentiostatic cathode control. Nernstian conditions for co-deposition must also be met, of course, whereby the metal ion activities are such that deposition potentials for the two metals become very close. The theory has been discussed elsewhere[13] and examples of its use reported. One such involves the stagewise recovery of silver, copper and gold in turn from a cyanide solution, arising in electronics/connector finishing. The waste solution contained 22.4 ppm Cu, 19 ppm Ag and 14.2 ppm Au. Because of the relative stabilities of the cyanide complexes, silver was recovered first at pH 4 and -0.55 V (MMS). On lowering the potential to -0.9 V, copper was recovered, after which the residual gold was deposited (see Fig. 4).

It is outside the scope of this lecture to discuss the way in which these concepts have been commercialized. It is appropriate to point out, however, that several successful products have been or are still available, having various degrees of sophistication, optimization and applicability—proprietary names include Ecocell,[14] Turbocel,[15] and Enthone-OMI.[16]

Process Simulation

Many electrochemical processes need to be simulated, each of which has specific characteristics and requirements. The most substantial examples of commercial high-speed electroplating are tinplate and electrogalvanizing. Three cell geometries are commonly employed, involving rapid strip movement through the electrolyte, either in serpentine cells or in horizontal cells; the reel-to reel technique is analogous,

Table 6
Conversion Factors in RCE Reactors

Reactor Mode	Conversion Factor, C_F
Simple batch	$\frac{C_t}{C_0} = \exp - kt$
Single pass	$\frac{C_{OUT}}{C_{IN}} = \frac{1}{1 + k\tau_R}$
Batch recycle	$\frac{C_{IN,t}}{C_{IN,0}} = \exp - \frac{t}{\tau}\left(1 - \frac{1}{1 + k\tau_R}\right)$
Cascade	$\frac{C_{OUT,n}}{C_{IN}} = \left(\frac{1}{1 + k\tau_R}\right)^n$

Table 7
Metal Recovery in a Series Operation

Cell No.	C_{in}, ppm	C_{out}, ppm	Overall Recovery, %*
1	100	50	50
2	50	25	75
3	25	12.5	87.5
4	12.5	6.25	93.8
5	6.25	3.125	96.9
6	3.125	1.563	98.4

* Assumes 100% current efficiency and 50% fractional conversion per cell-compartment

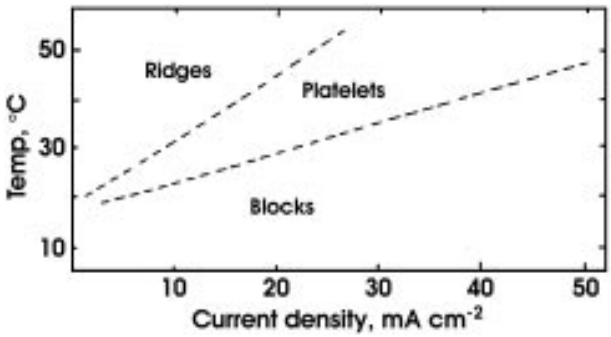

Fig. 7—Morphology diagram of temperature/current density for acid copper deposition (after Pick *et al.*).

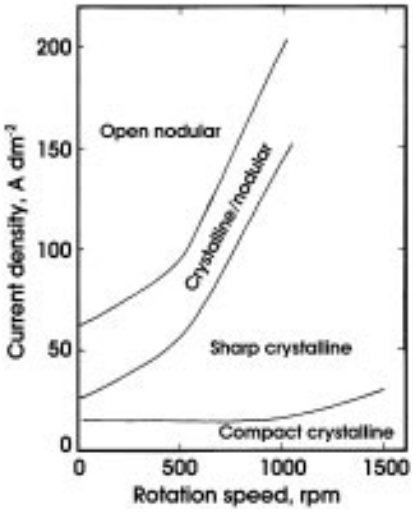

Fig. 9—Morphology diagram for zinc-nickel electrodeposits produced from an acid solution (after Wilcox and Gabe).

but used primarily in the electronics industry. Recent interest in radial cells offers some interesting advantages, but the essential feature in this discussion is that marked turbulent agitation is created, thereby increasing the limiting-current-density by at least an order of magnitude. An analogous process is the electroforming of foil, typically for printed circuit board applications.

Traditionally, control is by means of the Hull cell or one of its simple variants that are generally static or only moderately agitated. This gives a "static" current density range related to the industrial strip plating process by a "dynamic" multiplying factor obtained by experience, empirical interpolation or statistical correlation. Although these techniques have long been used and found to be generally adequate for addition agent control, provided the bright or leveled ranges

Table 8
Estimated Mass Transfer Coefficients

Rotation rate rpm	Method of estimation	Mass transfer coefficient cm s^{-1}
500	Equation a	2.2×10^{-4}
	Equation b	3.0×10^{-4}
5000	Equation a	1.1×10^{-3}
	Equation b	1.3×10^{-3}

Eq. a $Sh = 0.079\ Re^{0.7} Sc^{0.356}$

Eq. b $Sh = \frac{\Delta w}{Mt} \frac{1}{A} \frac{1}{(C_w - C_B)} \frac{d}{D}$

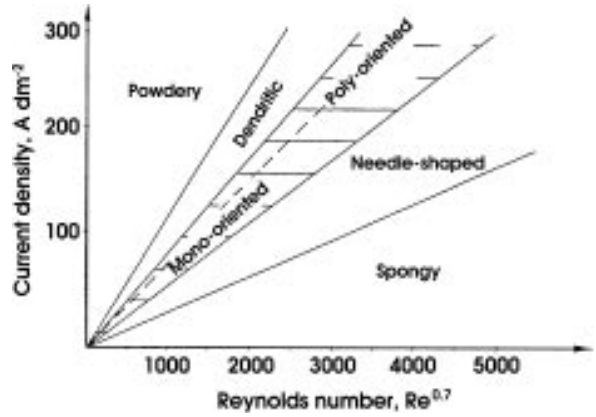

Fig. 8—Morphology diagram for acid zinc in terms of current density and Reynolds number (after Azzeri *et al.*).

of current density are wide, as is often the case, closer control is desirable as an aspect of improved quality control. The recent developments in "dynamic" Hull cell design have been referred to earlier in the context of RCE and RConE applications and have been discussed elsewhere recently by the author,[17] so will not be further explored here.

The quantitative basis for process simulation was first described in detail by Wranglen,[18] who considered a range of options, notably tube flow, but concluded that rotating electrodes are easily the preferred type (in his case, for corrosion studies). Using his approach, we may use an equivalence of mass-transfer performance as the point of equality and express it as two dimensionless Sherwood numbers for, say, an electrolytic tinning line (ETL) and the RCE. Accordingly, we equate

$$Sh_{ETL} = Sh_{RCE}$$

Mass transfer correlations for each cell geometry may be defined for turbulent flow:

$$Sh_{ETL} = 0.023\ Re^{0.8}\ Sc^{0.33}$$

$$Sh_{RCE} = 0.079\ Re^{0.67}\ Sc^{0.33}$$

from which we may obtain by equating

$$\log Re_{ETL} = 0.67 + 0.833 \log Re_{RCE}$$

Consequently, we obtain equivalent flow velocity terms in a common (turbulent) flow regime.

This type of analysis must be the basis of any simulation approach and the consequences may now be considered. Quantitative correlations have only rarely been reported and two may be cited: Heitz *et al.*[19,20] used both RCE and RDE techniques in comparison with tube flow in corrosion studies and obtained good correlations, apparently irrespective of the flow regime (see Fig. 5). Silverman[21] also studied corrosion processes and correlated numerically the mass transfer behavior with conventional weight loss measurements. The correlation was good and is given in Table 8. Equivalence through electrodeposition morphology is probably better documented, but less precise; it is being considered separately.

Electrodeposit Morphology Diagrams

Electrocrystallization theory can be traced to three strands of tradition and research. The Bulgarian school of Kaishew has

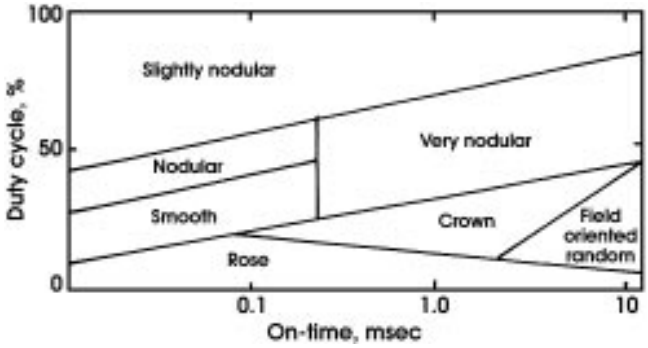

Fig. 10—Morphology diagram of on-time/duty cycle at 6 A/cm² and 55 °C for pulsed jet (Re = 12,000) plated gold contact spots (after Bocking).

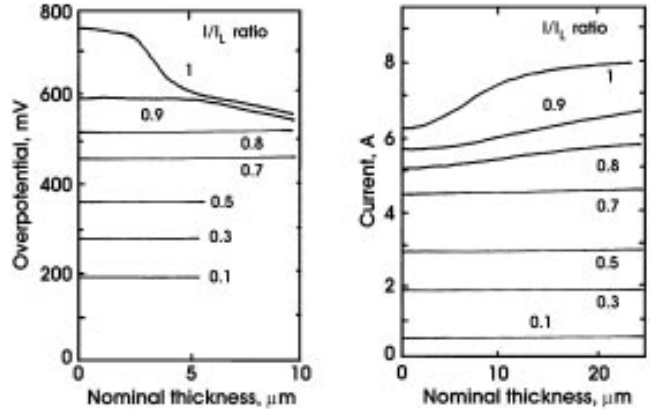

Fig. 11—Electrodeposition at fractions of the limiting current for acid copper sulfate solutions, using the RCE: (a) overpotential/nominal thickness at 900 rpm; (b) current/nominal thickness at 300 rpm (after Robinson and Gabe).

been concerned primarily with the metal physics of crystal nucleation and growth and has drawn analogy with condensation processes. The German school of Fischer has regarded crystallization as essentially a practical problem of morphology development and therefore to be related to the usual electroplating parameters, notably current or current density, and the consequent mechanical properties developed in the deposit. The school of Bockris has approached electrocrystallization as an exercise in electrochemical thermodynamics and therefore driven by Gibbs free energy (*i.e.*, electrode overpotentials). Each strand is credible, is best for its particular realm of relevance and can explain the well-established surface structure types in general terms of polarization parameters of potential and current density (Fig. 6).[22]

The concept of *Morphology Diagrams* can probably be attributed to Fischer[23] and a number of manifestations has been proposed, according to the specific need. The object is to use a two-variable graph in the simplest form to indicate the type of deposit morphology or surface structure that may arise on electrodepositing a coating to a thickness sufficient to yield a structure of "steady state" character. Each such graph will be characteristic of that metal and that solution, and no generalization for all metals and solutions can yet be made, although analogous behavior can often be discerned. Using acid copper solutions, Pick *et al.*[24] developed morphology diagrams (Fig. 7) for low currents or potentials, where deposition is agreed to be under activation control. Such diagrams suffered from a number of limitations; first, they were not clearly related to the practical problem of maximizing the current employed before roughening, leading to occurrence of powdery or dendritic growth. Second, they did not include a parameter of agitation, which in practice is employed not only to eliminate solution stagnation, but also to promote mass transfer and thereby develop high-speed deposition processing.

Two approaches can be made to these shortcomings. First, *morphology diagrams* can be introduced, using an agitative parameter for one axis, and electrode rotation rate is an obvious such parameter to quantify a form of mass transfer equivalence. Such diagrams have been constructed for a number of metals, and the RCE is at its best in these circumstances because of the relatively large surface area at uniform current density, which can afterward be examined by electron microscopy, as well as being subjected to a range of mechanical and other tests:

Alkaline zinc	Naybour[25]
Acid zinc	Azzerri et al.[26]
Cyanide gold	Vanhumbeeck *et al.*[27]
Palladium-nickel	Vanhumbeeck *et al.*[27]

Figure 8 (after Azzerri *et al.*) is illustrative of these approaches. In such diagrams, terminology varies so that primary growth implies flat, leveled or crystallographic formats; tertiary growth implies dendritic or powdery surfaces. Zone boundaries cannot be defined precisely because of the nature of the metallographic data, but we may note that zone boundaries should only be straight with a log-log graphical plot. This has been substantiated by Naybour's data for zinc. When alloy electrodeposition is employed, and especially if one metal is co-depositing under mass-transfer control and the other not, flow rate may affect the composition of the deposit. In this circumstance, deposit composition can be used as a factor of equivalence—a number of workers have made a preliminary attempt to do this, including Tseda *et al.*[28] with alloy deposits for Zn-Ni, using flow patterns of several types arising from superimposed jetting on flow. More recently, Gabe and Wilcox[29] have investigated other zinc alloys, (*e.g.*, Zn-Mn), but have not yet been able to control the process adequately to develop a product as a composition-modulated or a structure-modulated alloy. They have, however, constructed a morphology diagram for Zn-Ni alloy electrodeposits (see Fig. 9).

Pulse plating techniques have also been used in an analogous manner to modify both structural and physical properties of deposits.

Table 9
Critical Current Density Parameter Values

Metal	Solution	Log i_o (A/cm²)	i/i_L ratio for onset of dendritic growth
Copper	acid sulfate	-5/-4	0.4 - 0.7
Gold	alkaline cyanide		0.6
Iron	acid sulfate	-9/-8	0.8 - 0.9
Lead	acid perchlorate	-4	
Nickel	acid sulfate	-9/-8	0.9 - 1.0
Silver	acid nitrate	-1/-2	0.2
Tin	acid sulfonate	-3	0.4
Zinc	acid sulfate/chloride	-5/-3	
	alkaline zincate		0.4

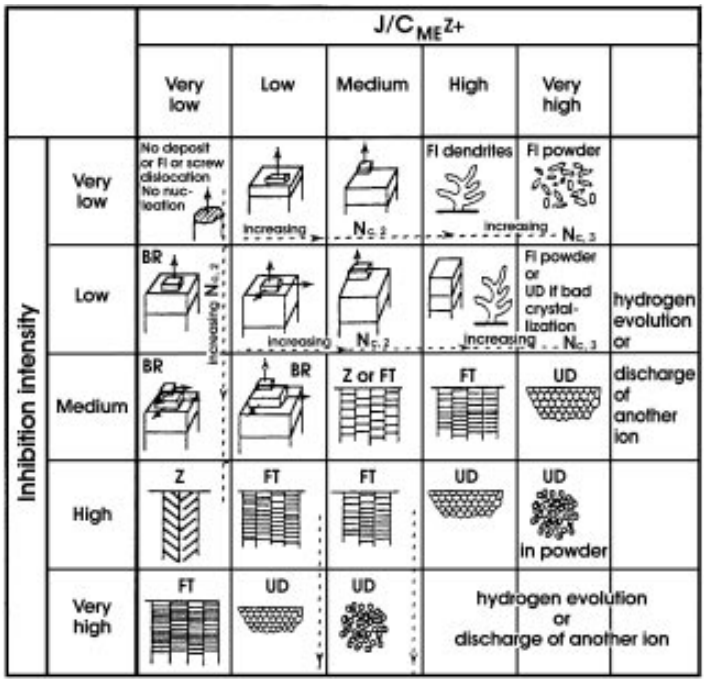

Fig. 12—Morphology diagram showing different types of polycrystalline electrodeposits (after Winand).

Bocking[30] has developed morphology diagrams using the pulse parameters of duty cycle and on-off time. A typical diagram is given as Fig. 10, in which more detailed structure analysis has been attempted.

A second approach arises when it is recognized that each metal/solution couple has its own character regarding morphology development. In relation to dendritic growth initiation, it is possible to introduce the i/i_L ratio as a criterion. Robinson and Gabe[31] suggested that for acid copper solutions, the ratio took a value of 0.7 when deposit thicknesses were ~5 μm; it is obvious that if statistical considerations are introduced, other ratio values may arise (*i.e.*, if one waits long enough, dendrites will always appear, usually as a result of some special instance of heterogeneous nucleation), so a lower limit ratio value may also be used, typically 0.4 for deposit thicknesses in excess of 20 μm. This manifests itself when polarization characteristics are measured as a function of time. In Fig. 11, potential/time and current/time graphs have been used to identify the onset of roughness. In this comparison, time has been converted to nominal thickness as a more practical parameter.

Such a criterion, being mass-transfer defined through the limiting current density i_L, does not take into account metal identity in the context of the electrode interface. This can best be done by means of the exchange current density i_o, which is characteristic for a particular metal/metal ion combination. West has suggested an approach to this relationship in which he equates activation and concentration polarization equations to obtain a derived equation for the critical current density ratio:[32]

$$(i/i_L)_{crit} = \{(1-i_o/i)_{crit}\}^{x/1-B}$$

Such a relationship suggests that $(i/i_L)_{crit}$ is smaller for larger values of i_o, which is a generally observed trend, and correlation of data reveals that a systematic behavior can be seen (Table 9). Winand[33] has revived the original concept of Fischer for this purpose and employed the i/i_L ratio together with an inhibitive intensity (possibly i_o) for his morphology diagrams (Fig. 12). This represents the nearest to a generalized diagram that has yet been achieved and effectively combines the kinetic and diffusive theories to best effect. This approach is the best option available at present to design an electroplating solution and process from first principles, taking into account the needs of both speed of deposition and quality of deposit. The approach appears credible; now we need an improved bank of data beyond that given in Table 9 that serves to demonstrate just how little information of this type seems to be available in the literature.

Acknowledgments

The work described in this lecture could only have been completed with the willing collaboration of many former colleagues and research students, as well as the financial and technical support of a number of sponsors, all of whom have contributed to the research program on *High Speed Electrodeposition.* These are listed in recognition and appreciation of their contributions.

Len Beard, Laurence Warner and Syd Melbourne;
Doug Robinson, Bob Ollerenshaw, Derek Carbin and Paul McBurney;
Frank Walsh, Geoff Wilcox, Jomi Makanjuola, Arjang Afshar, Majid Kalantary, Mehrdad Kalantary, Stephen Amadi and Chris Bocking;
Norman Gardner, Bev Sewell, Mark Goodenough, Ian Christie, Patrizia Micelli and Susanna Ramundo.
The Universities of Sheffield and Loughborough;
The Steel Company of Wales Ltd. and British Steel Corporation;
Athlone Fellowship and Commonwealth Scholarship Foundations;
Science and Engineering Research Council;
Ecological Engineering Ltd. (formerly of Macclesfield);
Twickenham Plating Group Ltd., London;
European Economic Community;
Centro Sviluppi Materiali spA, Rome;
G.E.C.-Marconi Hirst Research Centre, London.

References

1. D.A. Swalheim, *Trans. Electrochem. Soc.*, **86**, 395 (1944).
2. A.K. Graham and H.L. Pinkerton, *Proc. Amer. Electropl. Soc.*, **50**, 135 (1963).
3. D.R. Gabe, *J. Appl. Electrochem.*, **4**, 91 (1974).
4. D.R. Gabe and F.C. Walsh, *J. Appl. Electrochem.*, **13**, 3 (1983).
5. D.R. Gabe, F.C. Walsh, G.D. Wilcox *et al., J. Appl. Electrochem.*, 1996 (to be published).
6. A.F.S. Afshar, D.R. Gabe and B. Sewell, *Trans. Inst. Met. Fin.*, **69**, 37 (1991).
7. D. Landolt, C. Madore, M. Matlosz *et al., J. Appl. Electrochem.*, **22**, 1155 (1992); *Electrochim. Acta*, **37**, 69 (1992); *Plat. and Surf. Fin.*, **80**, 73 (Nov. 1993).
8. D-T. Chin, *J. Electrochem. Soc.*, **118**, 1434 (1971).
9. F.C. Walsh and D.R. Gabe, *I. Chem. E. Symp.*, **116**, 219 (Ser. 1990).
10. F.C. Walsh and D.R. Gabe, *Trans I. Chem. E.*, **68 B**, 107 (1990).
11. F.C. Walsh, N.A. Gardner and D.R. Gabe, *J. Appl. Electrochem.*, **12**, 299 (1982).

12. P.A. Makanjuola and D.R. Gabe, *Surface Technol.*, **24**, 29 (1985); *J. Appl. Electrochem.*, **17**, 370 (1987).
13. D.R. Gabe and F.C. Walsh, *Surface Technol.*, **12**, 25 (1981).
14. F.S. Holland, *Chem. Ind., London,* UK, 1978; p. 453.
15. J-Cl. Puippe, *Oberflach. Surf.*, **32**(2), 17 (1991); EAST Report 1990, 38, E.G. Leuze Verlag, Saulgau, Germany.
16. D. Hemsley, *Prod. Fin.*, **46**(9), 5 (1993); **47**(5), 6 (1994); **47**(7), 9 (1994).
17. D.R. Gabe, Plenary Lecture, Asia-Pacific Interfinish, Melbourne, (Oct. 1994).
18. G. Wranglen, J. Berendson and G. Karlberg, *Physiochemical Hydrodynamics* (B. Spalding, Ed.), Adv. Pubs., London, UK, 1977.
19. E. Heitz, *Werkstoff Korr.*, **15**, 63 (1964).
20. E. Heitz, G. Kreysa and C. Loss, *J. Appl. Electrochem.*, **9,** 243 (1979).
21. D.C. Silverman, *Corrosion,* **40,** 220 (1984).
22. D.R. Gabe, *Principles of Metal Surface Treatment and Protection,* 3rd Ed., Merlin Books, Devon, UK, 1993.
23. H. Fischer, *Elektrolytische Abscheidung und Elektrokristallization von Metallen,* Springer Verlag, Berlin, 1954.
24. H.J. Pick, G.G. Storey, T.B. Vaughan and S.C. Barnes, *Electrochim. Acta,* **2,** 165, 179, 195 (1960).
25. R.D. Naybour, *J. Electrochem. Soc.*, **116,** 520(1969); *Electrochim. Acta.*, **13**, 763 (1968).
26. S. Alota and N. Azzerri, *Proc. Corrosion 85* (NACE), Paper No. 386, Boston, 1985; *Proc. SURTEC 85,* 367, Berlin (1985).
27. J. Vanhumbeeck, *Proc. AESF SUR/FIN '84, Session C* (1984); F. Vangaever and J. Vanhumbeeck, *Proc. INTERFINISH 84,* 184, Jerusalem (1984); R. de Doncker and J. Vanhumbeeck, *Proc. Connectors 85,* 63, Leicester, UK (1985); R. de Doncker and J. Vanhumbeeck, *Trans. Inst. Met. Fin.*, **62,** 59 (1985).
28. Tseda *et al., Proc. AESF SUR/FIN '84,* Session C (1984).
29. D.R. Gabe and G.D. Wilcox (to be published).
30. C.C. Bocking, PhD Thesis, Loughborough University of Technology (1994).
31. D.R. Gabe and D.J. Robinson, *Trans. Inst. Met. Fin.*, **48,** 35 (1970); **49**, 17 (1971).
32. J.M. West, *Electrodeposition and Corrosion Processes,* 2nd Ed., Van Nostrand Reinhold, London, 1971.
33. R. Winand, *J. Appl. Electrochem.*, **21,** 377 (1991).

About the Author

Dr. David R. Gabe, recipient of AESF's 1994 Scientific Achievement Award (the most prestigious award presented by the Society), delivered the 36th William Blum Lecture on Monday, June 26, the opening day of SUR/FIN® '95—Baltimore. The text presented here is an edited version of his lecture.

Dr. Gabe is director of the Institute of Polymer and Materials Engineering at Loughborough (England) University of Technology, where he directs a substantial and diversified effort in metal finishing. He is a graduate of the University of Wales (Cardiff) and received a PhD from the University of Sheffield, England. Dr. Gabe's mailing address is IPTME, University of Technology, Loughborough, Leicestershire, England LE11 3TU.